Proceedings of the ASME 2014 4th Joint US-European Fluids Engineering Division Summer Meeting
FEDSM2014
August 3-7, 2014, Chicago, Illinois, USA

FEDSM2014-22089

INVESTIGATION OF EXHAUST CONDITIONS ON INFLUENCING CONTAMINANT TRANSPORT FOR INDOOR ENVIRONMENTS

Z. C. Zheng
University of Kansas
Lawrence, KS, USA

Z. Wei
University of Kansas
Lawrence, KS, USA

J.S. Bennett
National Institute for Occupational Safety and Health
Centers for Disease Control and Prevention
Cincinnati, OH, USA

ABSTRACT

Indoor air quality is an important issue involved in a wide variety of industrial applications. In an indoor environment, different types of contaminants exist and have an inevitable potential to cause health problems for human beings and animals. In this study, the focus is on the contaminant contained in painting materials. While painting materials being sprayed to solid surfaces, pollutant plumes are formed near the painting area, which may enclose the body parts of the sprayers. Severe health problems are possible to occur if a significant amount of painting materials settles on the face of workers. By applying exhaust conditions (i.e. exhaust fan with outlet velocity), the flow convection in the room can be enhanced, which may alleviate the contaminant level on the human body. In such a case, the choice of exhaust condition becomes crucial. With the aid of computational fluid dynamics, an optimal exhaust condition can be determined. To simulate this kind of fluid/solid-particle multiphase flow, the current study employs a pure Eulerian or Euler-Euler type model. In the Euler-Euler approach, the properties of the contaminant particles are assumed to be continuous as those of fluids and all phases are computed in the Eulerian framework. Since the exhaust speed is moderately low and fully turbulent flow is not guaranteed in the room, the RNG k-e model is used as a low Reynolds number turbulent model. The current paper firstly investigated the scenario of sprayer self-contamination. Then, inter-contaminations among different workers will be studied.

NOMENCLATURE

ρ	density, kg/m^3
Y_i	local mass fraction of each species
$\mathbf{u}$	velocity vector of flow field, m/s
$\mathbf{u_p}$	velocity vector of particles, m/s
$D_{i,m}$	diffusion coefficient of each species, m^2/s
μ_t	turbulent viscosity of flow field, kg/m-s
μ	laminar viscosity of flow field, kg/m-s
$\mathrm{Sc_t}$	turbulent Schmidt number
$\mathbf{F_D}$	the drag force per unit particle mass, m/s^2
C_D	the drag coefficient of particles
$\mathbf{F_b}$	the additional acceleration term of the DPM Model, force per unit particle mass, m/s^2
$\mathbf{g}$	the gravitational force, m/s^2

INTRODUCTION

The ventilation is of pivotal importance for the indoor environment in a painting hanger with presence of small particles coming out of painting sprays. In the present study, the working environment of a painting hanger to conduct helicopter painting is concerned. Workers are in the midst of painting pollution that has to be protected from to insure their health. In such an environment, the ventilation system needs to be substantiated to increase convection of the indoor air and transport contaminants outside of the hanger. Therefore, the control of exhaust speed becomes

important. A very high speed ventilation consumes too much energy and may not be necessarily effective, while a low speed ventilation cannot provide sufficient ventilation.

In order to study this problem, a numerical simulation is developed to simulate the fluid/particle multiphase flow in the painting hanger. The pure Eulerian interaction model is often employed for industrial applications [1]. It computes all phases in the Eulerian framework that is easy to use and requires relatively less computational resources. Some previous studies validated such a multiphase method against experimental works, i.e. [2, 3]. Also, modifications are made for pure Eulerian models to perform better in particular situations [4-6].

The current study adopts a pure Eulerian multiphase in a commercial CFD solver [7]. We are interested in the concentration of species transport in an indoor environment around a large object, i.e., a model helicopter. The influence of the exhaust velocity is carefully investigated.

SPECIES TRANSPORT EQUATIONS

For the i^{th} species, the conservation equation, Eq. (1), is computed for the concentration distributions of each species:

$$\frac{\partial}{\partial t}\left(\rho Y_i\right)+\nabla\bullet\left(\rho\mathbf{u}Y_i\right)=\nabla\bullet\left[\left(\rho D_{i,m}+\frac{\mu_t}{\mathrm{Sc}_t}\right)\nabla Y_i\right] \quad (1)$$

Here, ρ is the density of the mixture of all species, and Sc_t is the turbulent Schmidt number related to turbulent diffusivity and is selected as 0.7. In most practical applications, turbulent diffusion often overwhelms laminar diffusion. Since the mass fractions of the species must sum to unity, Eq. (2) is solved only for the first (N-1) species where N is the total number of continuous phase species in the system. In the current study, air and the tracer gas are the only two species. Therefore, the density of the mixture is obtained by the "volumetric-weighted mixing law".

$$\frac{1}{\rho}=\frac{Y_{air}}{\rho_{air}}+\frac{1-Y_{air}}{\rho_{tracer}} \quad (2)$$

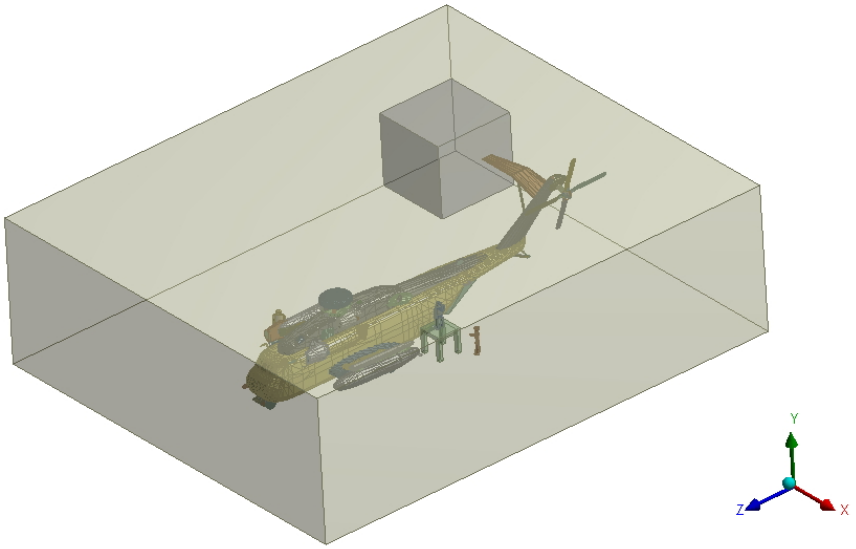

Figure 1- The geometry

GEOMETRY AND BOUNDARY CONDITIONS

Figure 1 shows the sketch of the geometry in the current study. The dimension of the outer domain is 28.118m × 9.8806m × 33.492m. The small cube near the z = 0 plane represents a control room, which does not allow flow to go in. Its dimension is 5.2518m × 4.88315m × 6.2518m. There are three groups of workers represented in Fig. 1. The first two groups consist a sprayer and a helper and the third group only has a sprayer. The model for workers is shown in Fig.2.

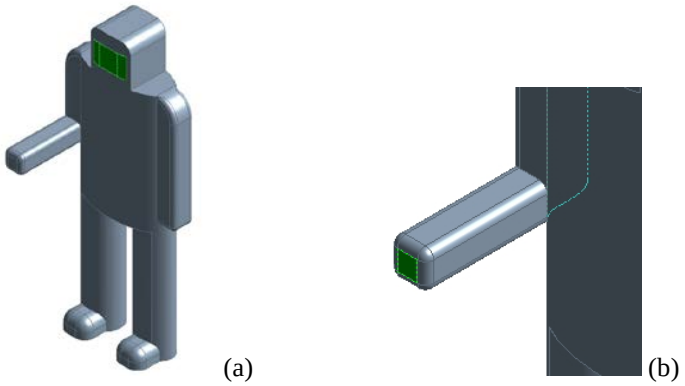

(a) (b)

Figure 2 - The geometry of the workers.
(a) The full scale model. The face region is highlighted (b) The detailed view of the hand. The injection region is highlighted

The species is injected from the hand of the sprayers, as shown in Fig. 2 (b). Figure 3 exhibits the locations of the workers. The injection plane is approximately parallel to the surfaces of the helicopter; thus, the species is blown perpendicular to the surfaces. Helpers are located downstream of the corresponding sprayers; they are 1m away and facing 45 degree towards the sprayers in terms of the z-direction. The sprayer #1 stands on a 2m table, yet the helper #1 is on the ground. Both sprayer #2 and helper #2 are on the ground. The sprayer #3 is lying on the ground and underneath the helicopter.

The speed of injection is 10m/s. In order to correctly specify the inlet boundary condition of the hanger ventilation system, the outlet boundary condition (z = 0 plane) is tuned to avoid reversed flow. The targeted inlet speeds include 100, 75 and 50 feet per minute (fpm). Since the inlet velocity is not high enough to ensure a fully turbulent flow, the RNG k-ε model is employed as a low Reynolds number turbulent model. Other details on the boundary conditions are listed in Table 1. The boundary conditions for the turbulence model are calculated based on turbulent flow through a channel [7]. The computational grid has approximately 1.9e7 total number of cells, and parallel computations are performed with 16 cores.

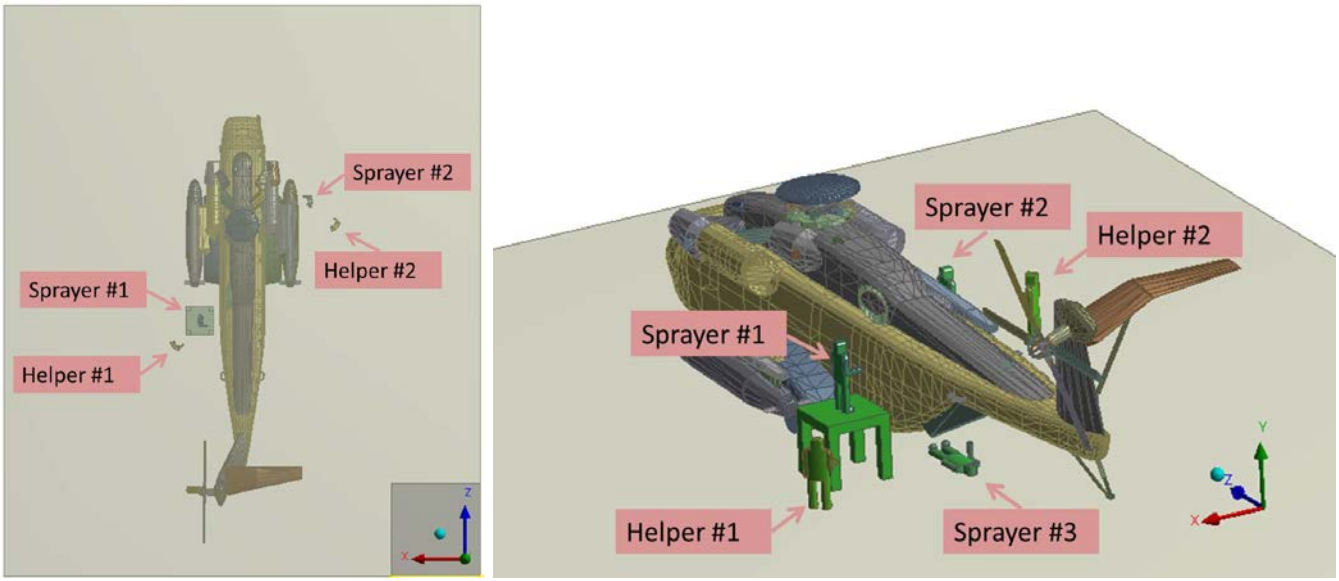

Figure 3 Location of the workers (a) x-z plane (b) back view

Table 1- Boundary conditions for all simulations

Boundary	B.C.	Momentum	Turbulence	Species Mass Fraction
Inlet (z = max)	Pressure Inlet	p = 0	Turbulence Intensity = 4.25(%) Turbulence Length Scale = 1.167(m)	0
Outlet (z = 0)	Inlet	Velocity Magnitude	Turbulence Intensity = 4.25(%) Turbulence Length Scale = 1.167(m)	0
Other Walls (x = 0 or max y = 0 or max)	Wall	Stationary, No slip		0 diffusive flux
Injection plane	Inlet	Velocity Magnitude = 10(m/s)	Turbulence Intensity = 4.22(%) Turbulence Length Scale = 4.389e-3(m)	1
Worker, Table and Helicopter Surfaces	Wall	Stationary, No slip		0 diffusive flux

RESULTS AND DISCUSSION

The cases with different inlet speeds are, firstly, simulated in the steady state condition. The convergence criterion is 10e-4 for all the cases. The influence from each of the sprayers is represented in Fig. 4 with different colors for concentration mole fraction iso-surfaces. The yellow color is for the injection from sprayer #1, purple for sprayer #2 and teal for sprayer #3. It can be seen that the size of the species plumes increases as the exhaust speed decreases. The species plume primarily encloses the corresponding group of workers. However, at very low speed, i.e. 50 fpm, the yellow plume also touches sprayer #3, a phenomenon not shown in higher ventilation speed cases. This indicates that higher exhaust speed can prevent such an 'inter-contamination' from happening.

However, no observable inter-contamination exists in the pictures in the Fig. 5, which has a higher iso-surface value. This implies that the contamination most occurs in the vicinity of the sprayers by paint injection from the sprayers themselves, and the different ventilation speeds do not make much difference.

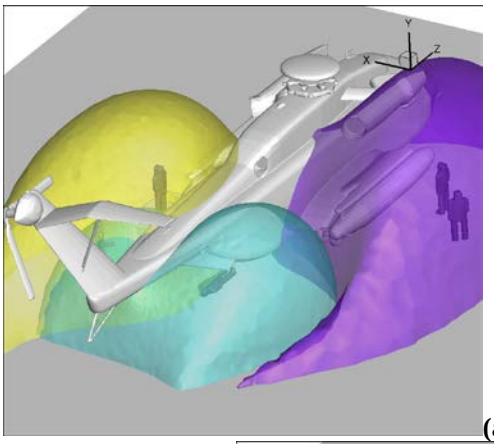

(a)

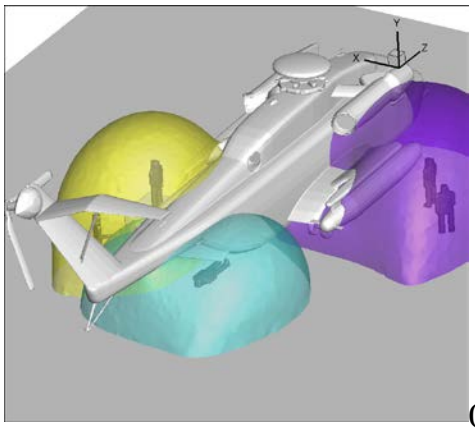

(b)

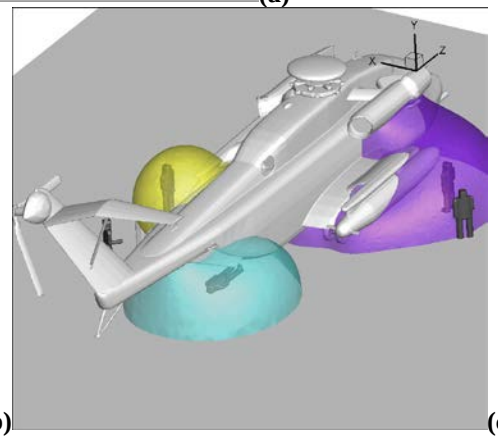

(c)

Figure 4 - Comparison of cases with different speeds. Iso-value of mole fraction is 0.01. [(a) 50 fpm; (b) 75 fpm; (c) 100 fpm]

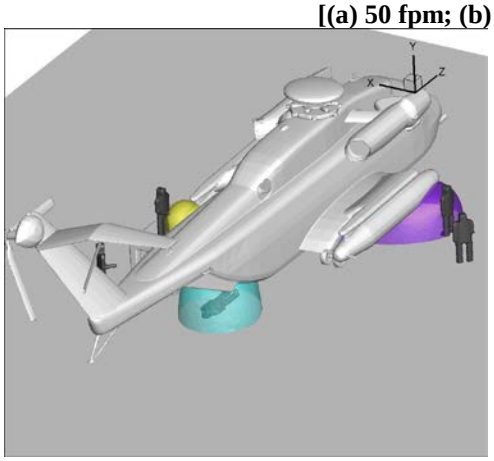

(a)

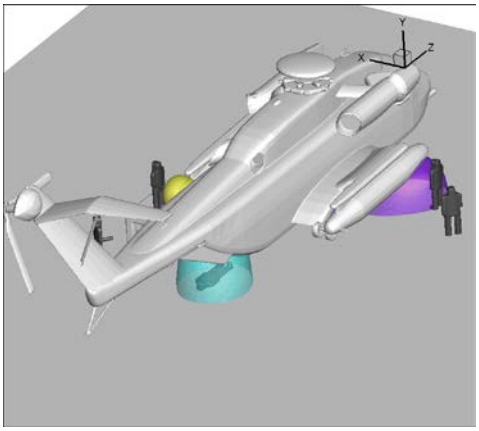

(b)

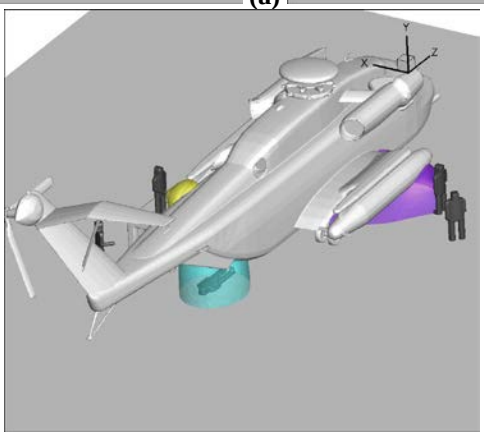

(c)

Figure 5- Comparison of cases with different speeds. Iso-value of mole fraction is 0.03. [(a) 50 fpm; (b) 75 fpm; (c) 100 fpm]

After converged to 10^{-4}, the steady simulations are further carried out with more strict convergence criteria of continuity, i.e. 10^{-5}. The histories of the species concentration are plotted in Fig. 6. The mole fractions at time = 0 represent that from the steady solutions. Similar to steady simulation, the unsteady simulation results demonstrate that the workers are mostly contaminated by the corresponding sprayers, yet the inter-contamination is detected. For example, in Fig. 6(e), the primary contamination source of sprayer #3 is sprayer #3 itself, which is called 'self-contamination'. However, the influence of sprayer #1 on sprayer #3 is not negligible. Fortunately, this inter-contamination is relatively small and reduces as the exhaust speed increases. Furthermore, curves in Fig. 6 clearly show that the position at sprayer #3 is most dangerous. This is reasonable since sprayer #3 is lying underneath the helicopter, in which the flow convection is reduced substantially.

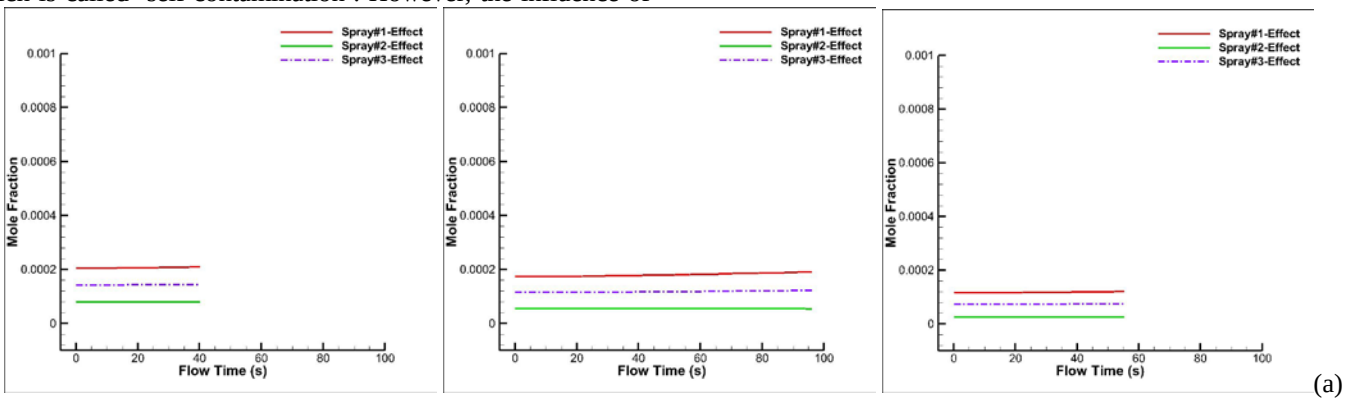

(a)

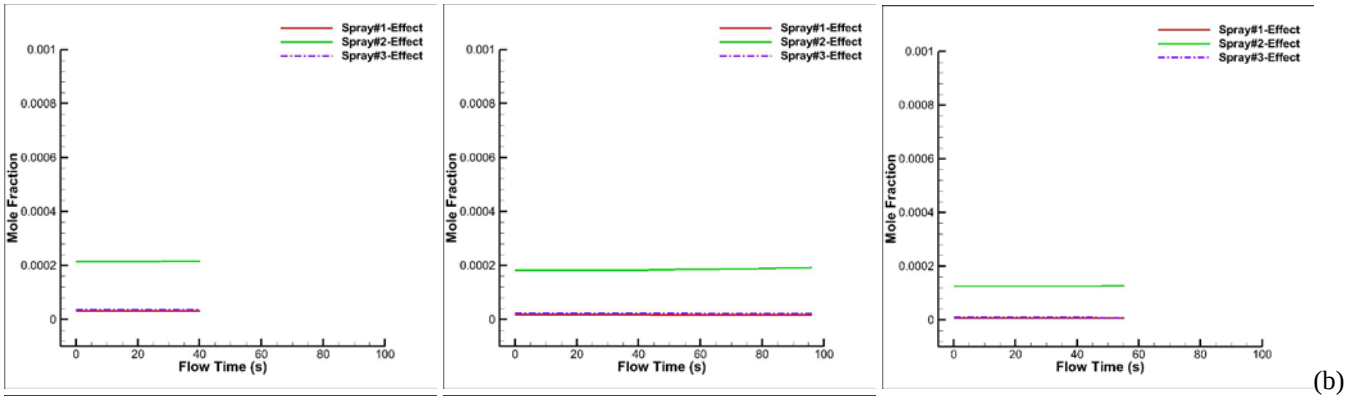

(b)

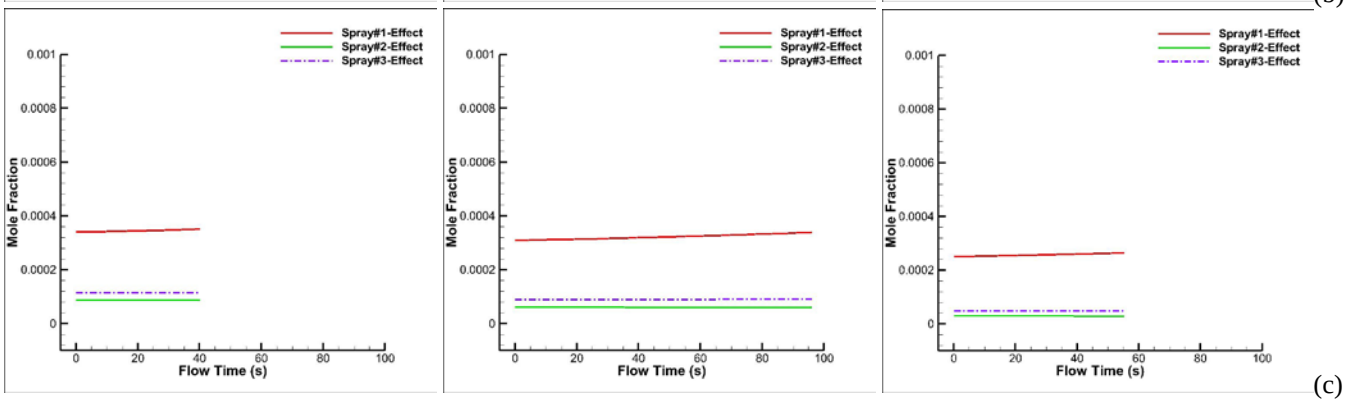

(c)

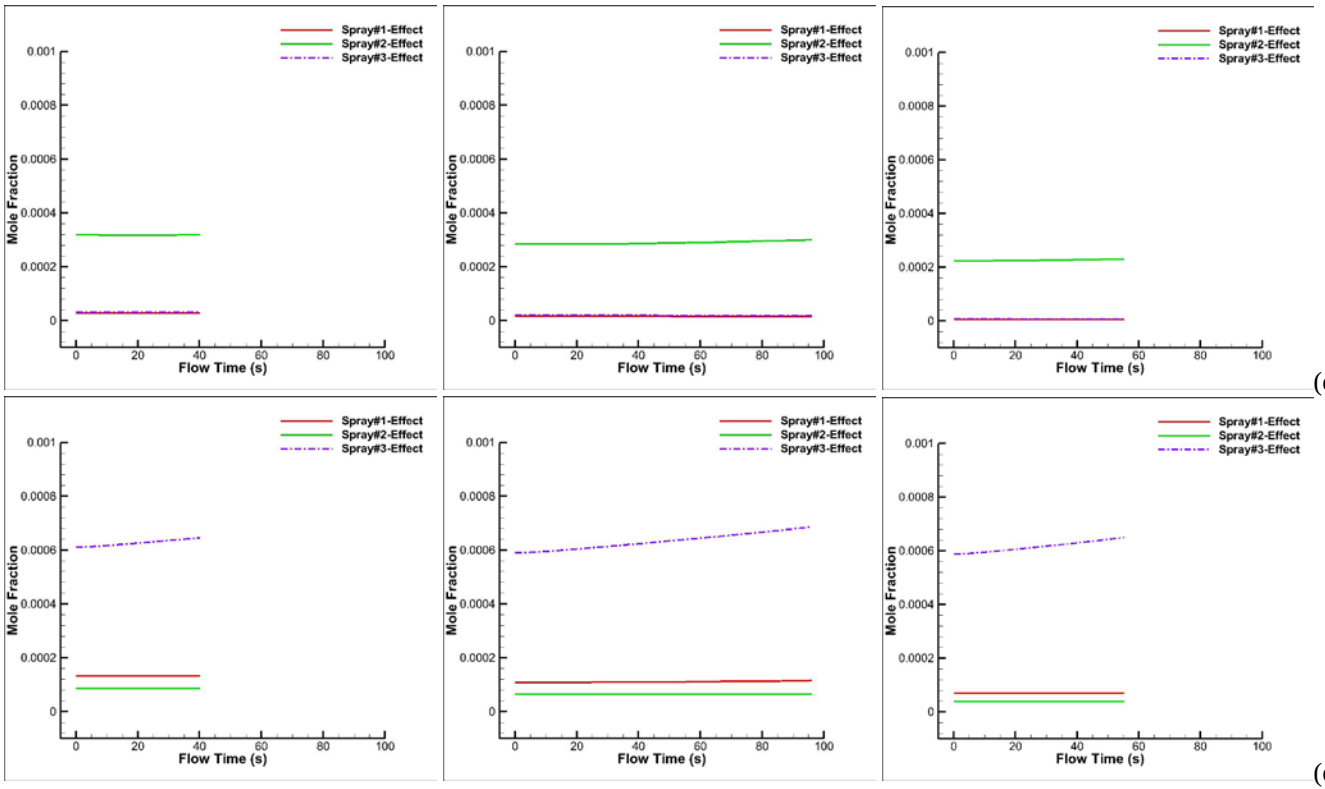

Figure 6 – Histories of species concentrations on the face of workers. (Left: 50 fpm; Middle: 75 fpm; Right: 100 fpm.) (a) helper #1 (b) helper #2 (c) sprayer #1 (d) sprayer #2 (e) sprayer #3

Another interesting phenomenon regarding the position at sprayer #3 is that the self-contamination is not reduced as the exhaust speed increases, although that happens to other workers in Fig. 6 (a)~(d), too. To further investigate this phenomenon, the sprayer #3-effect in Fig. 6(e) for different exhaust speeds is extracted and combined into Fig. 7. It is found that, even in the steady simulation, the case with 75 fpm does not perform worse than that with 100 fpm. In addition, as the unsteady simulation continues, the self-contamination of sprayer #3 in the case with 100 fpm becomes worse than that with 75 fpm. This indicates that the 75 fpm speed is a good potential alternative exhaust speed, since it has the possibility to not only achieve a similar or better performance of cleaning contamination from the faces of the workers, but also require less energy consumption.

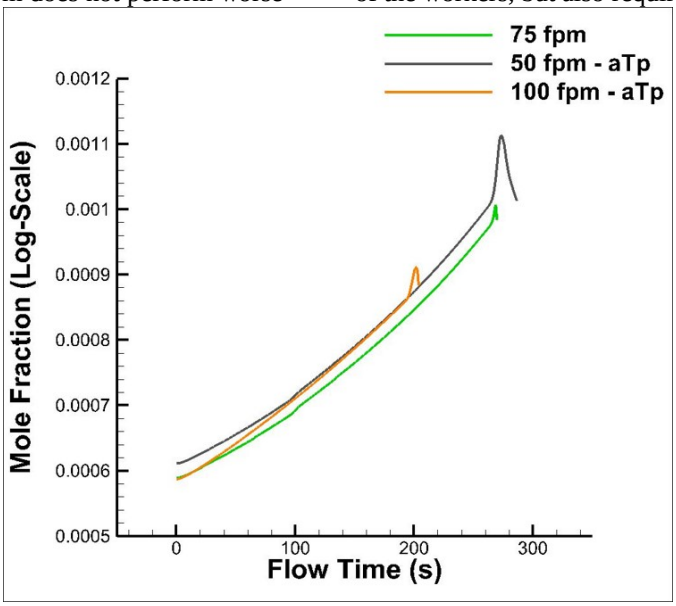

Figure 7 Histories of species concentrations for the self-contamination of sprayer #3

CONCLUSION AND RECOMMENDATIONS

This research has demonstrated the importance of the choice of the exhaust speed in order to maintain an acceptably safe indoor environment for painting workers in an aircraft hangar. The higher speed, i.e. 100 fpm, in general performs better, yet a medium speed, i.e. 75 fpm, can possibly achieve comparable performances. At this lower speed, a significant amount of energy can be saved. Future studies should be concentrated on the unsteady simulation, since the species concentration displayed in Fig. 7 is not converged to certain values yet.

ACKNOWLEDGMENTS

The first two authors acknowledge the support of CDC under the contract 200-2013-M-56348.

REFERENCES

[1] Ebrahimi, R., Zheng, Z. C., and Hosni, M. H., 2013, "A Computational Study of Turbulent Airflow and Tracer Gas Diffusion in a Generic Aircraft Cabin Model," ASME J. Fluids Eng., 135(111105).

[2] Lai, A. C. K., Wang, K., and Chen, F. Z., 2008, "Experimental and numerical study on particle distribution in a two-zone chamber," Atmos Environ, 42(8), pp. 1717-1726.

[3] Sun, W., Ji, J., Li, Y. G., and Xie, X. J., 2007, "Dispersion and settling characteristics of evaporating droplets in ventilated room," Build Environ, 42(2), pp. 1011-1017.

[4] Zhang, N., Zheng, Z. C., Glasgow, L., and Braley, B., 2010, "Simulation of particle deposition at the bottom surface in a room-scale chamber with particle injection," Adv Powder Technol, 21(3), pp. 256-267.

[5] Zhang, N., and Zheng, Z. C., 2007, "A collision model for a large number of particles with significantly different sizes," J Phys D Appl Phys, 40(8), pp. 2603-2612.

[6] Zhang, X. Y., and Ahmadi, G., 2005, "Eulerian-Lagrangian simulations of liquid-gas-solid flows in three-phase slurry reactors," Chem Eng Sci, 60(18), pp. 5089-5104.

[7] ANSYS, I., ANSYS® FLUENT, Release 14.0, Help System.

[8] Tian, L., and Ahmadi, G., 2007, "Particle deposition in turbulent duct flows - comparisons of different model predictions," J Aerosol Sci, 38(4), pp. 377-397.

[9] Shulman, S. A., Bennett, J. S., Sieber, W. K., MKatzoff, M. J., Wouhib, A., and Adams, B., 2006, "Estimating Tracer Gas Distribution in a Ventilation Chamber," International Biometric Society - ENAR - ASA Biometrics Section.

Disclaimer: The findings and conclusions in this paper have not been formally disseminated by the National Institute for Occupational Safety and Health and should not be construed to represent any agency determination or policy.